Projection of accurate configuration-interaction wave functions for He**
and the alkaline-earth-metal atoms onto simple rotor-vibrator wave functions

John E. Hunter III and R. Stephen Berry

Department of Chemistry and The James Franck Institute, The University of Chicago, Chicago, Illinois 60637

To quantify the extent of validity of the molecular model of atoms with correlated electrons, we project well-converged configuration-interaction wave functions for doubly excited states of He and for bound states of alkaline-earth-metal atoms onto simple rotor-vibrator wave functions for the "linear triatomic molecule" e-core-e. The three independent vibrational frequencies and the equilibrium electron-nucleus separation are treated as parameters which are varied to maximize the overlap with the well-converged functions. For intrashell states, the overlaps with harmonic normal-mode functions are generally quite large, about 85–95 % for the alkaline-earth-metals, and the corresponding optimized parameters are in rough agreement with the energy-level separations. The overlaps are improved by using an anharmonic local-mode representation, particularly for intershell states (corresponding to excited stretching vibrations), though the optimized parameters appear to lose some of the consistency shown by those in the harmonic normal-mode representation. A comparison is made of plots of the conditional probability densities based on rotor-vibrator functions and on independent-particle functions with those based on accurate functions. This shows clearly the superiority of the molecular picture over the independent-particle picture as a zero-order model for intrashell states of two-electron atoms.

I. INTRODUCTION

Since the first recognition of a clear breakdown of the independent-particle model in the spectrum of doubly excited helium (He**),[1,2] there have been extensive investigations of the nature of electron correlation in two-electron atoms. It became clear that the individual orbital angular momenta of the electrons were not good quantum numbers and thus that a search for alternative quantization would be desirable. In recent years two approaches have emerged, each with its associated new classification: the adiabatic hyperspherical picture[3] and the molecular picture;[4,5] these have been connected to some extent recently by Watanabe and Lin.[6] Here we focus on the molecular picture in which the atom e-core-e is viewed as a "linear triatomic molecule" whose characteristic quantum numbers are those describing rotational or vibrational excitations. This picture was originally suggested[4,7] on the basis of energy-level spacings in He** and was furthered by the finding[8,9] that reduced probability densities in the internal e-core-e coordinate system calculated from accurate configuration-interaction (CI) wave functions were qualitatively like those expected for a floppy linear triatomic molecule. The molecular picture was extended to the ground and low-lying bound excited states of the alkaline-earth-metal atoms by similar analyses of both energy-level spacings[10] and wave functions.[11]

Here we develop a quantitative characterization for this heretofore qualitative, intuitive picture of electron correlation. We do so by projecting well-converged CI wave functions for He** and the alkaline-earth atoms onto the corresponding simple rotor-vibrator wave functions of the "triatomic molecule" e-core-e; the parameters of the molecular function are varied to maximize the overlaps. We then examine the resulting parameters for their consistency with the observed energy-level spacings. How well can a *single* rotor-vibrator function (separable into the product of a function depending on the internal coordinates and a function of the Euler angles specifying the orientation of the e-core-e triangle in space) represent the accurate CI wave function? Can the wave functions of an entire manifold of states for a given atom be fit well and with a single sensible set of parameters? These are some of the questions which this paper seeks to address. The calculation of such overlaps is a crucial step in quantifying the extent of validity of the molecular picture and especially in seeing how well it can be extended to atoms with three or more valence electrons. The graphical representations that have been so useful in establishing the correspondence of the actual atomic states with their molecular analogues cannot readily be extended to cases of more than two electrons.

The rest of this paper will proceed as follows. In Sec. II we outline the forms of the atomic and molecular wave functions used, their transformation into a common coordinate system, and the calculation of the overlaps. Details are given in the appendices. Results for the harmonic normal-mode representation are presented in Sec. III A and those for various local-mode and anharmonic representations are discussed in Sec. III B. Concluding remarks are given in Sec. IV.

II. COORDINATE SYSTEM AND WAVE FUNCTIONS

The greatest difficulty in the calculation of the overlaps arises from the required transformation of the atom-

ic and molecular wave functions into a common coordinate system. This transformation is facilitated by an appropriate choice for the body-fixed reference frame $x'y'z'$. We have chosen the so-called bisector frame. The nucleus (effectively located at the center of mass) lies at the origin and the e-core-e triangle is chosen to lie in the $x'z'$ plane, with the x' axis bisecting the angle θ_{12} between the two radius vectors. Thus when the "molecule" is exactly linear, it lies along the body-fixed z' axis in agreement with the usual convention. Stated mathematically,

$$\hat{\mathbf{x}}' = \frac{\hat{\mathbf{r}}_1 + \hat{\mathbf{r}}_2}{|\hat{\mathbf{r}}_1 + \hat{\mathbf{r}}_2|} , \tag{1a}$$

$$\hat{\mathbf{y}}' = \frac{\hat{\mathbf{r}}_1 \times \hat{\mathbf{r}}_2}{|\hat{\mathbf{r}}_1 \times \hat{\mathbf{r}}_2|} , \tag{1b}$$

$$\hat{\mathbf{z}}' = \hat{\mathbf{x}}' \times \hat{\mathbf{y}}' , \tag{1c}$$

where $\hat{\mathbf{r}}_1$ and $\hat{\mathbf{r}}_2$ are unit vectors in the directions of the two electrons. In the harmonic normal-mode approximation, the molecular rotor-vibrator (RV) wave function may be written as[12-14]

$$\Psi_{RV} = \mathcal{A} \frac{1}{r_1 r_2} R_{v_1 v_3}(r_1, r_2) G_{v_2}^k(\theta_{12})$$
$$\times \left[\frac{2J+1}{8\pi^2} \right]^{1/2} \mathcal{D}_{Mk}^{J*}(\alpha\beta\gamma) , \tag{2}$$

where

$$R_{v_1 v_3}(r_1, r_2) = \mathcal{N} e^{-(q_1^2 + q_3^2)/2} H_{v_1}(q_1) H_{v_3}(q_3) , \tag{3}$$

$$G_{v_2}^k(\theta_{12}) = \mathcal{N} \rho_2^{|k|} e^{-\rho_2^2/2} L_{(v_2 - |k|)/2}^{|k|}(\rho_2^2) , \tag{4}$$

$$q_1 = \sqrt{m_e \omega_1/2\hbar}(\Delta r_1 + \Delta r_2) , \tag{5}$$

$$\rho_2 = \sqrt{m_e \omega_2/2\hbar}(\pi - \theta_{12}) r_e , \tag{6}$$

$$q_3 = \sqrt{m_e \omega_3/2\hbar}(\Delta r_1 - \Delta r_2) , \tag{7}$$

$$\Delta r_i = r_i - r_e . \tag{8}$$

The quantum numbers v_1, v_2, and v_3 specify, respectively, the number of quanta in the three normal modes of vibration: the symmetric stretch, the (doubly degenerate) bend, and the antisymmetric stretch; q_1, ρ_2, and q_3 are the corresponding dimensionless normal coordinates and ω_1, ω_2, and ω_3 are the corresponding vibrational frequencies. J is the total angular momentum (excluding spin) and M is its projection on the space-fixed z axis; k is the vibrational angular momentum about the body-fixed z' axis. $\mathcal{D}_{Mk}^J(\alpha\beta\gamma)$ is a rotation matrix (in the convention of Brink and Satchler[15]), whose arguments are the Euler angles which effect the transformation from the space-fixed frame to the body-fixed frame, m is the electron mass, and r_e is the equilibrium electron-nucleus separation. $\mathcal{A}$ is the antisymmetrization operator. $H_n(x)$ is an Hermite polynomial and $L_n^\alpha(x)$ is an associated Laguerre polynomial in the convention of Gradshteyn and Ryzhik.[16] The $\mathcal{N}$'s are normalization

constants; they must be determined directly by evaluating the appropriate normalization integrals (e.g., $\int_0^\infty dr_1 \int_0^\infty dr_2 [R_{v_1 v_3}(r_1, r_2)]^2 = 1$) instead of using conventional formulas, since the usual approximation of very small amplitude motion does not hold rigorously here. Note that the stretching function is simply a product of harmonic oscillator functions in q_1 and q_3 and that the bending wave function is that of a two-dimensional harmonic oscillator. The factor of $1/(r_1 r_2)$ is introduced so that the wave function can be normalized over the same radial volume element as that for the atomic wave function (i.e., $r_1^2 r_2^2 dr_1 dr_2$).

By using pseudopotentials, the alkaline-earth atoms can be treated as quasi-two-electron atoms; thus the wave functions for both He and the alkaline earths can be written in the same form. The two-electron atomic CI wave functions we have employed here are those from Refs. 9 and 11. They are of the form
form

$$\Psi_{CI} = \mathcal{A} \sum_{l_1 n_1 l_2 n_2} C_{l_1 n_1 l_2 n_2} \phi_{n_1 l_1}(r_1) \phi_{n_2 l_2}(r_2) \mathcal{Y}_{l_1 l_2}^{LM}(\hat{\mathbf{r}}_1, \hat{\mathbf{r}}_2) , \tag{9}$$

where the radial basis functions are

$$\phi_{nl}(r) = \mathcal{N} r^{n-1} e^{-\xi r}, \quad n > l \tag{10}$$

and the angular basis functions are coupled spherical harmonics

$$\mathcal{Y}_{l_1 l_2}^{LM}(\hat{\mathbf{r}}_1, \hat{\mathbf{r}}_2) = \sum_{m_1 m_2} Y_{l_1 m_1}(\theta_1, \varphi_1) Y_{l_2 m_2}(\theta_2, \varphi_2)$$
$$\times \langle l_1 m_1 l_2 m_2 | LM \rangle . \tag{11}$$

The quantum numbers here have their usual meanings. Using a method outlined in detail by Nikitin and Ostrovsky,[17] the coupled spherical harmonics can be transformed into a form depending on θ_{12} and the Euler angles

$$\mathcal{Y}_{l_1 l_2}^{LM}(\hat{\mathbf{r}}_1, \hat{\mathbf{r}}_2) = \sum_K (-1)^{M+K} F_{l_1 l_2}^{LK}(\theta_{12}) \mathcal{D}_{-MK}^L(\alpha\beta\gamma) , \tag{12}$$

where

$$F_{l_1 l_2}^{LK}(\theta_{12}) = \sum_{m_1 m_2} Y_{l_1 m_1}(\theta_1', \varphi_1') Y_{l_2 m_2}(\theta_2', \varphi_2')$$
$$\times \langle l_1 m_1 l_2 m_2 | L - K \rangle \tag{13}$$

and (θ_i', φ_i') are the spherical polar coordinates of electron i in the body-fixed frame. With our choice of coordinate system as described above,

$$(\theta_1', \varphi_1') = \left[\frac{\pi}{2} - \frac{\theta_{12}}{2}, 0 \right] , \tag{14a}$$

$$(\theta_2', \varphi_2') = \left[\frac{\pi}{2} + \frac{\theta_{12}}{2}, 0 \right] . \tag{14b}$$

Explicit expressions for the particular $F_{l_1 l_2}^{LK}(\theta_{12})$'s that

we used are listed in Appendix A along with useful symmetry relations for these functions. Now substituting Eq. (12) into Eq. (9), Ψ_{CI} can be written as a function of the same coordinates as Ψ_{RV}.

After a moderate amount of algebra outlined in Appendix B, which uses the orthogonality of the rotation matrices with different values of J, k, and M, we find that

$$\langle \Psi_{RV} \mid \Psi_{CI} \rangle = (-1)^{L+S}(1+\delta_{k0})^{-1/2} \left[\frac{8\pi^2}{2L+1} \right]^{1/2} \delta_{LJ}\delta_{\pi_a \pi_m}$$

$$\times \sum_{l_1,n_1,l_2,n_2} C_{l_1 n_1 l_2 n_2} \int_0^\pi (\sin\theta_{12})d\theta_{12} G_{v_2}^k(\theta_{12}) F_{l_1 l_2}^{LK}(\theta_{12})$$

$$\times \int_0^\infty r_1 dr_1 \int_0^\infty r_2 dr_2 R_{v_1 v_3}(r_1,r_2)[\phi_{n_2 l_2}(r_1)\phi_{n_1 l_1}(r_2)$$

$$+ \pi_a(-1)^{S+k}\phi_{n_1 l_1}(r_1)\phi_{n_2 l_2}(r_2)] , \qquad (15)$$

where $\pi_a = (-1)^{l_1+l_2}$ is the parity of the atomic wave function, $\pi_m = (-1)^{k+S+v_3}$ is the parity of the molecular wave function, and δ_{mn} is the Kronecker delta. We have assumed the M and S (total electron spin) quantum numbers of the two wave functions to be the same. One of the integrals over dr can be performed analytically in terms of the error function, leaving only the simpler product of two separable one-dimensional numerical integrations which we performed using Gaussian quadrature. The fraction of overlap is given by $|\langle \Psi_{RV} \mid \Psi_{CI} \rangle|^2$.

The correspondence between the atomic and molecular descriptions of the states considered here is given in Table I. In each case we choose the lowest state in a particular symmetry channel (cf. Ref. 11), regardless of its nominal configuration. This selection would be especially questionable for Ba, which we do not treat, and could possibly be so for Sr, but the results indicate that the correspondence is satisfactory in that case. This appears to be a good point at which to clarify a lingering confusion in the literature concerning "rotor states." The states with $L \neq 0$ clearly have angular momentum; however, they fall into two distinct types: in the lowest $^1P^o$ and $^3P^e$ the angular momentum is the vibrational angular momentum k about the molecular axis z', whereas for the $^3P^o$ and $^1D^e$ it corresponds to the angular momentum $J-k$ of end-over-end rotation about an axis

(y') perpendicular to the molecular axis. It is only the latter which are referred to as rotor states in the usual nomenclature of molecular physics.

We next calculate the overlaps between the corresponding atomic and molecular wave functions, and maximize these overlaps by varying the parameters ω_1, ω_2, ω_3, and r_e. Generally we obtain at least three significant figures in the optimization of the parameters. We have included only the alkaline-earth atoms up to Sr in our calculations. In Ba there is considerable uncertainty about the classification of states. In addition, the wave functions from Ref. 11 for Ba are of questionable accuracy since they include no core polarization or spin-orbit coupling effects.

In order to examine graphically the behavior of the various wave functions in their internal coordinates, we construct conditional probability densities[9] $\rho(r_2,\theta_{12} \mid r_1 = \zeta)$, which measure the probability of finding one electron at a distance r_2 from the nucleus with angle θ_{12} between the two r vectors given that the other electron is at $r = \zeta$. This is related to the integral of the absolute square of the wave function over all possible orientations in space (i.e., over the Euler angles). The calculation is somewhat involved for the atomic CI wave functions (see Ref. 9) but quite simple for the molecular wave functions since they are naturally in the appropriate coordinates. The plots we present represent

TABLE I. Connection between molecular and atomic quantum numbers. Note that the molecular J is equal to the atomic L. The nominal atomic configurations are given.

$n_1 l_1 n_2 l_2$	Term	$(v_1 v_2 v_3)$	J	k	$J-k$
$nsns$	$^1S^e$	(000)	0	0	0
$nsnp$	$^3P^o$	(000)	1	0	1
$npnp$	$^1D^e$	(000)	2	0	2
$nsnd$					
$ns(n-1)d$					
$nsnp$	$^1P^o$	(010)	1	1	0
$npnp$	$^3P^e$	(010)	1	1	0
$npnp$	$^1S^e$	(020)	0	0	0
$ns(n+1)s$	$^1S^e$	(100)	0	0	0
$ns(n+1)s$	$^3S^e$	(001)	0	0	0

$r_2^2\rho(r_2,\theta_{12}\mid r_1=\zeta)$. All of the plots are scaled to constant height.

III. RESULTS AND DISCUSSION

A. Harmonic normal-mode representation

In lowest order the energy levels of a linear triatomic molecule are given by[18]

$$E(v_1,v_2,v_3,J,k)=\omega_1(v_1+\tfrac{1}{2})+\omega_2(v_2+1)$$

$$+\omega_3(v_3+\tfrac{1}{2})+B[J(J+1)-k^2]\ , \quad (16)$$

where B is the rotational constant. By examining the experimental energy differences[19,20] between the atomic states corresponding to different rotational and vibrational excitations, we can arrive at the values for the ω_i's and r_e that should hold if the molecular picture were rigorously correct. In doing so we have taken $E(0,1,0,1,1)$ to be the average of the true energies of the k doublet $^1P^o$ and $^3P^e$, and the rotational constant B to be one half the energy difference between the vibrationless states with $J=0$ and 1 (see Ref. 10). The resulting values serve as our standard of comparison for the parameters obtained by maximizing the overlaps.

In examining the overlaps we begin with the intrashell states, which correspond to excitations of rotational and bending vibrational modes only, and thus are states dominated by angular correlations. The results are indicated in Table II where the parameters leading to the best overlaps are listed for each state considered. The overlaps appear reasonably large for He**, and even better for the alkaline-earth atoms. The states corresponding to the very lowest degrees of excitation are fit best, while some of those corresponding to two quanta of excitation (e.g., the $^1D^e$'s for the heavier alkaline-earth atoms and the $2p^2\,^1S^e$ for He) show the simple model already breaking down somewhat. There is a fair bit of consistency among the optimized parameters for the various states of each atom as well as reasonable agreement of the average parameters for each atom with the predicted values based on the level separations (see Table III). The decrease of the predicted vibrational frequencies in going from Be through Sr is well-reproduced by the calculated parameters. Internal consistency is also demonstrated in that the overlaps calculated using a single average set of parameters for each atom are only slightly lower than those calculated with the optimal parameters.

The aptness of the molecular functions as representations of the accurate functions, and their superiority over the independent-particle model functions, can be seen clearly in Fig. 1, where we plot accurate conditional probability densities for the various states of He** and compare them with those constructed using the molecular wave functions and with single-configuration hydrogenic wave functions. These plots are drawn for the value of the fixed r near that at the maximum of the single-particle radial distribution function of the CI functions. Note that the $^3P^e$ state is constrained by symmetry to look very much the same in the three levels of approximation considered; the others are not.

Next we move on to examine intershell states, which correspond to excited stretching vibrations which we might associate with strong radial correlation. These results are shown in Table IV. The harmonic normal-mode model appears to encounter difficulties. The overlaps are rather small, and there are large differences between the best-fit parameters for the symmetric and antisymmetric stretches ($^1S^e$ and $^3S^e$). The ω_i's are far from their predicted values and they do not agree well at all with those obtained from the overlaps for the intrashell states. It appears that the intershell states are too diffuse radially for the harmonic model to work well. The fit of the $^3S^e$'s is better since they are constrained by symmetry to have the proper form. The symmetric stretching motion, on the other hand, is in direct competition with the shell structure.

B. Alternative choices
for molecular wave functions

In light of the poor agreement for intershell states we considered using a local-mode representation for the stretching vibrations, based on the success of such a representation[21] for molecules such as H_2O in which there is a large difference in the constituent masses. In contrast to the normal-mode picture described above, where radial correlations are explicit, in the local-mode picture radial correlation is forced into the wave function only by the antisymmetrization constraint. Transforming to the local-mode representation corresponds to replacing $R_{v_1v_3}(r_1,r_2)$ in Eqs. (2) and (15) by another function which is now separable in r_1 and r_2,

$$R_{nm}^{\pm}(r_1,r_2)=\tfrac{1}{2}(2-\delta_{nm})^{1/2}[g_n(r_1)g_m(r_2)$$

$$\pm g_m(r_1)g_n(r_2)]\ , \quad (17)$$

where n and m are, respectively, the number of vibrational quanta in the two equivalent "bonds." In addition (±1) replaces $(-1)^{v_3}$ in all equations. In the harmonic approximation

$$g_n(r)=\mathcal{N}e^{-q^2/2}H_n(q)\ , \quad (18)$$

$$q=\sqrt{m_e\omega/\hbar}(r-r_e)\ . \quad (19)$$

We also considered Morse eigenfunctions[22] for the $g_n(r)$'s,

$$g_n(r)=\mathcal{N}e^{-z/2}z^{b/2}L_n^b(z)\ , \quad (20)$$

$$z=\kappa e^{-a(r-r_e)}\ , \quad (21)$$

$$b=\kappa-2n-1\ , \quad (22)$$

corresponding to the Morse potential

$$V(r)=D(e^{-2a(r-r_e)}-2e^{-a(r-r_e)})\ , \quad (23)$$

$$\kappa=2\sqrt{2mD}/a\hbar\ . \quad (24)$$

The number of bound states supported is the largest integer strictly less than $(\kappa+1)/2$ and the energy levels are given by

TABLE II. Molecular parameters leading to best overlaps of normal-mode molecular wave functions with the corresponding atomic CI wave functions for intrashell states of He** and the alkaline-earth atoms. Here and in the following tables the ω's are in Rydbergs and r_e is in bohr.

Atom	State	ω_1	ω_2	ω_3	r_e	$\|\langle \Psi_{RV} \| \Psi_{CI} \rangle\|^2$	$\|\langle \Psi_{RV} \| \Psi_{CI} \rangle\|^2_{avg}$
He	$2s2s\,^1S^e$	0.892	0.250	0.746	3.44	0.7784	0.7257
He	$2s2p\,^3P^o$	0.831	0.185	0.614	3.33	0.7984	0.7875
He	$2p2p\,^1D^e$	0.527	0.152	0.418	3.18	0.7583	0.7412
He	$2s2p\,^1P^o$	0.675	0.136	0.440	3.46	0.7864	0.7687
He	$2p2p\,^3P^e$	0.551	0.249	0.415	3.02	0.9262	0.8994
He	$2p2p\,^1S^e$	0.418	0.234	0.256	3.43	0.6537	0.5903
He	average	0.649	0.201	0.482	3.31	0.7836	0.7521
Be	$2s2s\,^1S^e$	0.953	0.223	0.835	2.50	0.9387	0.8945
Be	$2s2p\,^3P^o$	0.791	0.283	0.671	2.58	0.9228	0.9092
Be	$2p2p\,^1D^e$	0.502	0.241	0.319	3.00	0.7921	0.7626
Be	$2s2p\,^1P^o$	0.586	0.151	0.372	2.89	0.8402	0.8176
Be	$2p2p\,^3P^e$	0.575	0.286	0.417	2.79	0.9254	0.9115
Be	average	0.682	0.237	0.523	2.75	0.8838	0.8591
Mg	$3s3s\,^1S^e$	0.765	0.119	0.669	3.08	0.9414	0.8215
Mg	$3s3p\,^3P^o$	0.619	0.177	0.501	3.38	0.8881	0.8703
Mg	$3s3d\,^1D^e$	0.357	0.210	0.187	4.14	0.5796	0.5158
Mg	$3s3p\,^1P^o$	0.467	0.101	0.272	3.73	0.7357	0.7130
Mg	$3p3p\,^3P^e$	0.457	0.166	0.376	3.89	0.9327	0.9095
Mg	average	0.533	0.154	0.401	3.64	0.8155	0.7660
Ca	$4s4s\,^1S^e$	0.555	0.075	0.492	3.96	0.9429	0.8458
Ca	$4s4p\,^3P^o$	0.465	0.132	0.385	4.31	0.9040	0.8950
Ca	$4s3d\,^1D^e$	0.658	0.387	0.416	3.37	0.5240	0.4228
Ca	$4s4p\,^1P^o$	0.403	0.105	0.282	4.51	0.8220	0.7798
Ca	$4p4p\,^3P^e$	0.361	0.161	0.318	4.78	0.9394	0.8592
Ca	average	0.488	0.172	0.379	4.19	0.8265	0.7605
Sr	$5s5s\,^1S^e$	0.507	0.060	0.451	4.28	0.9448	0.8280
Sr	$5s5p\,^3P^o$	0.486	0.128	0.418	4.58	0.9348	0.9266
Sr	$5s4d\,^1D^e$	0.415	0.231	0.360	4.26	0.6847	0.6669
Sr	$5s5p\,^1P^o$	0.458	0.124	0.362	4.60	0.8960	0.8829
Sr	$5p5p\,^3P^e$	0.385	0.260	0.371	4.66	0.9001	0.7817
Sr	average	0.450	0.161	0.392	4.48	0.8721	0.8172

$$E_n = \frac{-a^2\hbar^2(\kappa-2n-1)^2}{8m} \, . \qquad (25)$$

For the local-mode wave functions the overlap integral is simplified since it is entirely separable in r_1, r_2, and θ_{12}. In maximizing the overlaps with these functions, we vary ω and r_e in the harmonic case, and a, κ, and r_e in the Morse case.

Before going to intershell states (which we expect to improve the most by this better representation), we consider the ground stretching state (i.e., intrashell states) in this local-mode representation. Using the harmonic model we obtain results nearly identical to those shown in Table II for the normal-mode case; the correspondence between the optimized stretching frequencies is $\omega \approx (\omega_1+\omega_3)/2$. Using the anharmonic Morse functions,

TABLE III. Comparison of zero-order harmonic predictions (based on experimental energy-level spacings) with the calculated average molecular parameters giving the best overlaps for intrashell states of He** and the alkaline-earth atoms.

Atom	ω_1 Pred.	ω_1 Calc.	ω_2 Pred.	ω_2 Calc.	ω_3 Pred.	ω_3 Calc.	r_e Pred.	r_e Calc.
He**	0.382	0.649	0.135	0.201	0.354	0.482	5.32	3.31
Be	0.498	0.682	0.366	0.237	0.475	0.523	2.23	2.75
Mg	0.396	0.533	0.324	0.154	0.375	0.401	2.24	3.64
Ca	0.304	0.488	0.214	0.172	0.287	0.379	2.68	4.19
Sr	0.279	0.450	0.194	0.161	0.265	0.392	2.73	4.48

the magnitude of the overlaps is greatly improved (see Table V), though the bending frequencies appear to be far too large and the parameters a and κ correspond to a Morse potential that supports *no* excited bound stretching states.

Turning to the overlaps for intershell states in the local-mode representation, we find the same problems with the harmonic approximation as we found with normal modes. With the Morse functions, however, the picture is much improved. The consistency between the parameters for the $^1S^e$ and $^3S^e$ is excellent (see Table VI) and the overlaps are quite large. As Table VII shows, there is good consistency between the values of $-E_0$ calculated from the best-fit parameters and the actual ion-

ization potentials, and fair agreement between the calculated and experimental energy separations [from $(\omega_1+\omega_3)/2$]. The excited stretching states lie quite close to the top of the well and thus sample extremely anharmonic parts of the potential (which supports no higher-stretching states). The bending frequencies however appear somewhat inaccurate and the parameters do not agree with those for the intrashell states. Thus we have not been able to arrive at a model that can describe both intrashell and intershell states well with a single set of parameters.

In order to graphically represent radial correlation, we plot in Fig. 2 the conditional probability densities $r_1^2 r_2^2 \rho(r_1,r_2 \mid \theta_{12}=\pi)$ constructed from wave functions in
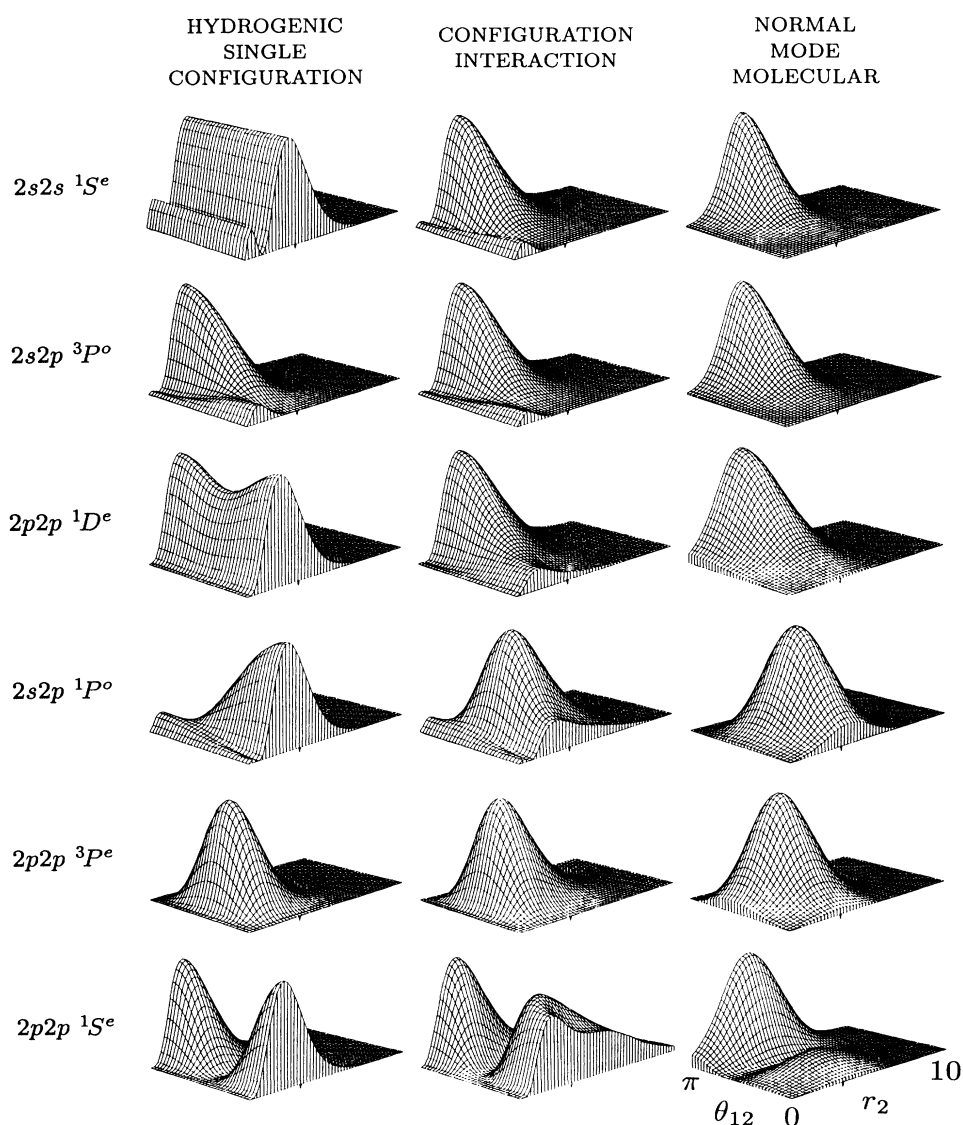
FIG. 1. Comparison of plots of conditional probability densities $r_2^2\rho(r_2,\theta_{12}\mid r_1=3)$ for intrashell states of He** constructed from the accurate CI wave functions (center column) and from two zero-order models—the single-configuration hydrogenic wave functions (left column), and the normal-mode molecular wave functions with optimized parameters (right column). The axes are all as indicated on the plot at the lower right. The position of the fixed electron is marked by a small tooth.

TABLE IV. Molecular parameters leading to best overlaps of normal-mode molecular wave functions with the corresponding atomic CI wave functions for intershell states of He** and the alkaline-earth atoms. No stable optimization was achieved for the $5s\,6s\ ^1S^e$ state of Sr.

Atom	State	ω_1	ω_2	ω_3	r_e	$\mid \langle \Psi_{RV} \mid \Psi_{CI} \rangle \mid^2$
He	$2s\,3s\ ^1S^e$	0.137	0.331	0.029	3.24	0.5114
He	$2s\,3s\ ^3S^e$	0.397	0.111	0.225	5.41	0.6907
Be	$2s\,3s\ ^1S^e$	0.200	0.083	0.003	2.59	0.7257
Be	$2s\,3s\ ^3S^e$	0.304	0.032	0.166	4.47	0.8274
Mg	$3s\,4s\ ^1S^e$	0.150	0.054	0.001	3.13	0.7060
Mg	$3s\,4s\ ^3S^e$	0.272	0.019	0.148	5.28	0.8197
Ca	$4s\,5s\ ^1S^e$	0.172	0.042	0.040	4.15	0.6979
Ca	$4s\,5s\ ^3S^e$	0.335	0.018	0.180	6.06	0.8894
Sr	$5s\,6s\ ^1S^e$					
Sr	$5s\,6s\ ^3S^e$	0.569	0.019	0.321	5.49	0.9521

TABLE V. Molecular parameters leading to best overlaps of Morse local-mode molecular wave functions with the corresponding atomic CI wave functions for intrashell states of He** and the alkaline-earth atoms.

Atom	State	a	ω_2	κ	r_e	$\mid \langle \Psi_{RV} \mid \Psi_{CI} \rangle \mid^2$	$\mid \langle \Psi_{RV} \mid \Psi_{CI} \rangle \mid^2_{av}$
He	$2s\,2s\ ^1S^e$	1.287	0.695	1.674	2.01	0.8867	0.8314
He	$2s\,2p\ ^3P^o$	1.190	0.570	1.721	1.89	0.8855	0.8722
He	$2p\,2p\ ^1D^e$	0.991	0.582	1.790	1.64	0.8160	0.7970
He	$2s\,2p\ ^1P^o$	1.159	0.475	1.639	1.83	0.8680	0.8438
He	$2p\,2p\ ^3P^e$	0.972	0.954	1.834	1.55	0.9881	0.9580
He	$2p\,2p\ ^1S^e$	1.091	1.157	1.559	1.55	0.7110	0.6533
He	average	1.115	0.739	1.703	1.75	0.8592	0.8260
Be	$2s\,2s\ ^1S^e$	1.059	0.654	2.118	1.46	0.9966	0.9682
Be	$2s\,2p\ ^3P^o$	1.086	0.962	1.944	1.40	0.9836	0.9771
Be	$2p\,2p\ ^1D^e$	1.141	1.179	1.609	1.36	0.8542	0.8252
Be	$2s\,2p\ ^1P^o$	1.211	0.693	1.612	1.34	0.9108	0.8848
Be	$2p\,2p\ ^3P^e$	1.069	1.225	1.763	1.35	0.9856	0.9716
Be	average	1.113	0.943	1.809	1.38	0.9462	0.9254
Mg	$3s\,3s\ ^1S^e$	0.872	0.306	2.235	1.91	0.9973	0.9160
Mg	$3s\,3p\ ^3P^o$	0.874	0.510	2.019	1.99	0.9505	0.9465
Mg	$3s\,3d\ ^1D^e$	1.074	0.999	1.467	1.90	0.6457	0.5683
Mg	$3s\,3p\ ^1P^o$	0.965	0.386	1.679	1.91	0.7970	0.7665
Mg	$3p\,3p\ ^3P^e$	0.726	0.470	2.098	2.31	0.9928	0.9567
Mg	average	0.902	0.534	1.900	2.00	0.8767	0.8308
Ca	$4s\,4s\ ^1S^e$	0.686	0.170	2.398	2.62	0.9963	0.9217
Ca	$4s\,4p\ ^3P^o$	0.635	0.308	2.344	2.80	0.9551	0.9117
Ca	$4s\,3d\ ^1D^e$	0.325	0.659	6.485	2.58	0.5236	0.4480
Ca	$4s\,4p\ ^1P^o$	0.604	0.269	2.247	2.80	0.8649	0.7774
Ca	$4p\,4p\ ^3P^e$	0.477	0.343	2.811	3.24	0.9783	0.8078
Ca	average	0.545	0.350	3.257	2.81	0.8636	0.7733
Sr	$5s\,5s\ ^1S^e$	0.624	0.127	2.519	2.91	0.9944	0.8779
Sr	$5s\,5p\ ^3P^o$	0.448	0.234	3.554	3.38	0.9629	0.9446
Sr	$5s\,4d\ ^1D^e$	0.458	0.495	3.207	2.91	0.7063	0.6796
Sr	$5s\,5p\ ^1P^o$	0.392	0.224	3.976	3.42	0.9163	0.8885
Sr	$5p\,5p\ ^3P^e$	0.271	0.413	6.529	3.70	0.9119	0.7645
Sr	average	0.439	0.299	3.957	3.26	0.8984	0.8310

TABLE VI. Molecular parameters leading to best overlaps of Morse local-mode molecular wave functions with the corresponding atomic CI wave functions for intershell states of He** and the alkaline-earth atoms.

Atom	State	a	ω_2	κ	r_e	$\|\langle \Psi_{RV} \| \Psi_{CI} \rangle\|^2$
He	$2s\,3s\;^1S^e$	0.609	0.434	3.531	2.50	0.8045
He	$2s\,3s\;^3S^e$	0.627	0.495	3.626	2.39	0.8691
Be	$2s\,3s\;^1S^e$	0.671	0.201	3.486	1.69	0.9102
Be	$2s\,3s\;^3S^e$	0.648	0.224	3.611	1.68	0.9587
Mg	$3s\,4s\;^1S^e$	0.586	0.120	3.499	2.13	0.9241
Mg	$3s\,4s\;^3S^e$	0.571	0.115	3.635	2.11	0.9648
Ca	$4s\,5s\;^1S^e$	0.455	0.091	3.981	2.97	0.9234
Ca	$4s\,5s\;^3S^e$	0.404	0.071	4.315	3.02	0.9578
Sr	$5s\,6s\;^1S^e$	0.387	0.122	4.870	3.39	0.7669
Sr	$5s\,6s\;^3S^e$	0.325	0.048	6.369	3.52	0.9684

various approximations for the $2s\,3s\;^1S^e$ and $2s\,3s\;^3S^e$ states of He. [We choose the value $\theta_{12}=\pi$ since this is clearly the maximum in the distributions $\rho(r_1,\theta_{12}\,|\,r_2 =\zeta)$ showing the angular correlation in these states.[9]] Figure 2 shows clearly the failure of the normal-mode picture to describe the excited symmetric stretch. The Morse local-mode picture does much better at reproducing the accurate density. But what is most striking here is that the best local-mode plot looks very much like the single-configuration hydrogenic plot, which in turn is very close to the accurate plot. That is, the independent-particle model appears to describe the bulk of the radial correlations, while the angular part is much better described by the molecular picture.

We have used three descriptions here for the stretching modes: the harmonic normal-mode model, the harmonic local-mode model, and an anharmonic local-mode model. A fourth model suggests itself, an anharmonic normal-mode description. Such a model can be constructed even though the normal modes lose their special, natural character if the anharmonic contributions to the energy are comparable with the harmonic, "off-diagonal" bond-bond contributions. Developing a normal-mode model or any more general optimized model for the two anharmonic stretching modes would require optimizing all the anharmonic parameters used to describe the system, and one would inevitably obtain

functions whose overlaps with the well-converged functions are at least as large as those reported here. Such functions would very likely be useful as basis functions for testing expansions of the exact eigenfunctions in terms of a rotor-vibrator series, instead of a series of independent-particle functions. If one were to develop stretching-mode functions for this purpose, one would surely want to start not with a pair of Morse potentials for the individual electron-nuclear interactions but with potentials that are asymptotically Coulombic. Indeed, such a step is part of the intended work of this program. However, it is not meant to be part of the stage presented here. The goal of this report is simply to show that for a great many of the states of common two-electron systems, there are simple rotor-vibrator representations that are much more like the exact eigenfunctions than the best independent-particle functions are. For this purpose the anharmonic, local-mode model based on Morse potentials is quite adequate.

Finally, we have also considered including anharmonicity in the angular part of the wave function. The angular functions used were Jacobi polynomials that result as an analytic approximation[23] to the eigenfunctions of two electrons confined to the surface of a sphere. These should do better at describing large-amplitude bending motion than the harmonic oscillator functions employed above. We will not give details here except to say that

TABLE VII. Comparison of predicted values of the stretching excitation energy and experimental ionization potentials with the calculated values based on the average molecular parameters giving the best overlaps for intershell states.

Atom	Av. params.		E_1-E_0		$-E_0$	
	a	κ	Pred.	Calc.	Pred.	Calc.
He**	0.618	3.579	0.368	0.603	0.554	0.635
Be	0.660	3.549	0.487	0.675	0.685	0.708
Mg	0.579	3.567	0.386	0.525	0.562	0.552
Ca	0.430	4.148	0.296	0.397	0.449	0.458
Sr	0.356	5.620	0.272	0.459	0.419	0.676

the resulting overlaps for intrashell states are very close to those given in Table II, and that the resulting average optimized parameters lead to bending energy-level separations which differ from the experimental values by percentages comparable to the percentage differences of the predicted and calculated ω_2 values given in Table III.

IV. CONCLUSION

We have shown that the molecular picture of an atom with two correlated electrons has the ability to describe well the wave functions of a whole group of intrashell states in both He** and the alkaline-earth atoms, with a few parameters that are reasonably well predictable from experimental energy-level separations. The molecular wave functions we have considered here have no explicit coupling between the angular and radial motions. The harmonic normal-mode functions give a rather good description of the intrashell states (rotation and bending vibrations) but fail for intershell states (symmetric and antisymmetric stretching vibrations). The most satisfactory representation of the states that would be assigned as stretching vibrations is given by suitably symmetrized Morse local-mode functions. The implication is clear that the effective potentials[24] do support vibrationlike behavior. However, in the radial direction this is so anharmonic that the normal modes associated with quadratic potentials have little application to the stretching modes of two-electron atoms apart from their correspondence with the correct symmetries. For high Rydberg states, the angular functions of the independent-particle model must be recovered.[25] Clearly a better understanding is still needed of the transition from independent-particle to collective-molecular behavior.

Now that the molecular picture has been placed on a more quantitative footing, it remains to establish its utility in making predictions of experimentally observable quantities. In particular we have in mind examining its implications for the angular distributions of photoelectrons (treated in analogy with photofragment angular distributions from molecular photodissociation).

ACKNOWLEDGMENTS
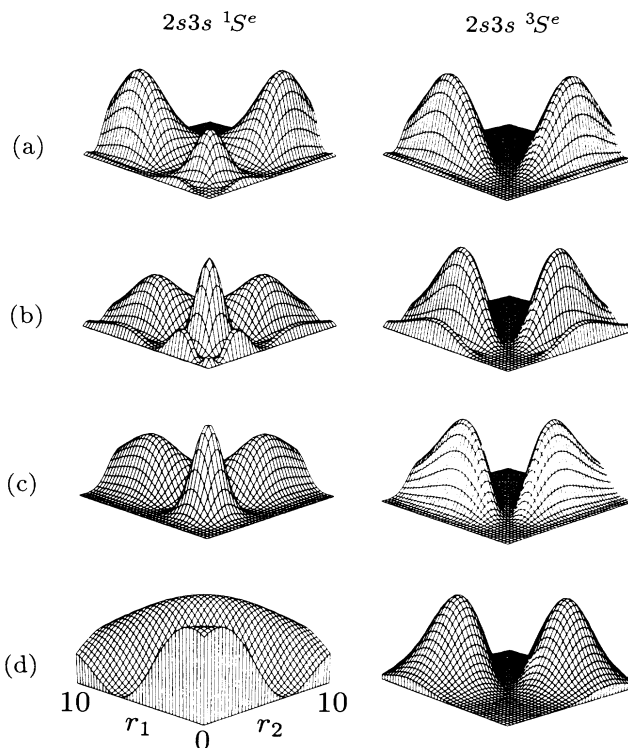
FIG. 2. Comparison of plots of conditional probability densities $r_1^2 r_2^2 \rho(r_1, r_2 \mid \theta_{12} = \pi)$ for the $2s3s\ {}^1S^e$ and $2s3s\ {}^3S^e$ states of He constructed from (a) the CI wave functions and from three zero-order models—(b) the single-configuration hydrogenic functions, (c) the Morse local-mode molecular wave functions with optimized parameters, and (d) the harmonic normal-mode molecular wave functions with optimized parameters. The axes are all as indicated on the plot at the lower left.

APPENDIX A: EVALUATION OF THE $F_{l_1 l_2}^{LK}(\theta_{12})$'s

In order to develop explicit expressions for the $F_{l_1 l_2}^{LK}(\theta_{12})$'s, we begin by rewriting their definition [Eqs. (13) and (14)] in terms of a 3-j symbol and define $u \equiv (\pi + \theta_{12})/2$,

$$F_{l_1 l_2}^{LK}(\theta_{12}) = (-1)^{l_1 + l_2 + K}(2L+1)^{1/2} \sum_m \begin{vmatrix} l_1 & l_2 & L \\ m & -m-K & K \end{vmatrix} Y_{l_1,m}(\pi-u,0) Y_{l_2,-m-K}(u,0) \ . \tag{A1}$$

Using symmetry relations for the spherical harmonics

$$Y_{lm}(\pi-\theta,0) = (-1)^{l+m} Y_{lm}(\theta,0) \ , \tag{A2}$$

$$Y_{lm}(\theta,0) = Y_{lm}^*(\theta,0) = (-1)^m Y_{l,-m}(\theta,0) \ , \tag{A3}$$

and for the 3-j symbols, the following relations may be determined directly:

$$F_{l_1 l_2}^{LK*}(\theta_{12}) = F_{l_1 l_2}^{LK}(\theta_{12}) \ , \tag{A4}$$

$$F_{l_2 l_1}^{LK}(\theta_{12}) = (-1)^{L+K} F_{l_1 l_2}^{LK}(\theta_{12}) \ , \tag{A5}$$

$$F_{l_1 l_2}^{L-K}(\theta_{12}) = (-1)^{l_1+l_2+L+K} F_{l_1 l_2}^{LK}(\theta_{12}) \ . \tag{A6}$$

Using the difference equations satisfied by the associated Legendre polynomials and their relationship with the spherical harmonics (see Ref. 26), it can be shown for general θ that

$$Y_{l+1,m}(\theta,0) = \left[\frac{(2l+3)(l-m)}{(2l+1)(l-m+1)} \right]^{1/2} \left[(\sin\theta)Y_{l,m+1}(\theta,0) + (\cos\theta) \left[\frac{l+m+1}{l-m} \right]^{1/2} Y_{l,m}(\theta,0) \right] \ , \tag{A7}$$

$$Y_{l+2,m}(\theta,0) = \left[\frac{(2l+5)(2l+3)}{(l+m+2)(l-m+2)} \right]^{1/2} \left[(\cos\theta)Y_{l+1,m}(\theta,0) - \left[\frac{(l+m+1)(l-m+1)}{(2l+1)(2l+3)} \right]^{1/2} Y_{l,m}(\theta,0) \right] \ . \tag{A8}$$

Explicit expressions for the 3-j symbols can introduce factors of m, m^2, or $[(l-m)(l+m+1)]^{1/2}$ into the summation in Eq. (A1). However, the sum may be carried out analytically using the following identities, which can be derived starting with the spherical harmonic addition theorem

$$\sum_m Y_{lm}(\pi-u,0)Y_{lm}(u,0) = \frac{2l+1}{4\pi} P_l(\cos\theta_{12}) \ , \tag{A9}$$

$$\sum_m m Y_{lm}(\pi-u,0)Y_{lm}(u,0) = 0 \ , \tag{A10}$$

$$\sum_m m^2 Y_{lm}(\pi-u,0)Y_{lm}(u,0) = \frac{2l+1}{8\pi} P_l^1(\cos\theta_{12}) \cot\frac{\theta_{12}}{2} \ , \tag{A11}$$

$$\sum_m [(l-m)(l+m+1)]^{1/2} Y_{lm}(\pi-u,0)Y_{l,m+1}(u,0) = -\frac{2l+1}{4\pi} P_l^1(\cos\theta_{12}) \ . \tag{A12}$$

Using all of the above results, the following explicit expressions were derived for the functions used in our calculations:

$$F_{ll}^{00}(\theta_{12}) = \frac{(-1)^l}{4\pi} (2l+1)^{1/2} P_l(\cos\theta_{12}) \ , \tag{A13}$$

$$F_{ll}^{11}(\theta_{12}) = \frac{(-1)^{l+1}}{4\pi} \left[\frac{3(2l+1)}{2l(l+1)} \right]^{1/2} P_l^1(\cos\theta_{12}) \ , \tag{A14}$$

$$F_{l,l+1}^{11}(\theta_{12}) = \frac{(-1)^l}{4\pi} \left[\frac{3}{2(l+1)} \right]^{1/2} \left[(l+1)\cos\left[\frac{\theta_{12}}{2} \right] P_l(\cos\theta_{12}) - \sin\left[\frac{\theta_{12}}{2} \right] P_l^1(\cos\theta_{12}) \right] \ , \tag{A15}$$

$$F_{l,l+1}^{10}(\theta_{12}) = \frac{(-1)^{l+1}}{4\pi} \left[\frac{3}{l+1} \right]^{1/2} \left[(l+1)\sin\left[\frac{\theta_{12}}{2} \right] P_l(\cos\theta_{12}) + \cos\left[\frac{\theta_{12}}{2} \right] P_l^1(\cos\theta_{12}) \right] \ , \tag{A16}$$

$$F_{ll}^{20}(\theta_{12}) = \frac{(-1)^{l+1}}{4\pi} \left[\frac{5(2l+1)}{(2l+3)(l+1)l(2l-1)} \right]^{1/2} \left[l(l+1)P_l(\cos\theta_{12}) - \tfrac{3}{2}\cot\left[\frac{\theta_{12}}{2} \right] P_l^1(\cos\theta_{12}) \right] \ , \tag{A17}$$

$$F_{l,l+2}^{20}(\theta_{12}) = \frac{(-1)^l}{4\pi} \left[\frac{15}{2(l+1)(l+2)(2l+3)} \right]^{1/2} \left\{ \left[(2l+3)(l+1)\sin^2\left[\frac{\theta_{12}}{2} \right] - (l+1)^2 \right] P_l(\cos\theta_{12}) \right.$$
$$\left. + \frac{1}{2} \left[(2l+3)\sin\theta_{12} + \cot\left[\frac{\theta_{12}}{2} \right] \right] P_l^1(\cos\theta_{12}) \right\} \ . \tag{A18}$$

APPENDIX B: CALCULATION OF THE OVERLAPS

First we obtain explicitly antisymmetrized wave functions by applying the operator

$$\mathcal{A} = 1 + (-1)^S \hat{P}_{12} \tag{B1}$$

to the expressions for the wave functions given in the text [Eqs. (2) and (9)]. $\hat{P}_{12}$ is the permutation operator,

$$\hat{P}_{12} R_{v_1 v_3}(r_1,r_2) = (-1)^{v_3} R_{v_1 v_3}(r_1,r_2) \ . \tag{B2}$$

With our choice of the body-fixed frame,

$$\hat{P}_{12} \mathcal{D}_{Mk}^J(\alpha,\beta,\gamma) = \mathcal{D}_{Mk}^J(\alpha-\pi,\pi-\beta,2\pi-\gamma) \tag{B3}$$

$$= (-1)^J \mathcal{D}_{M-k}^J(\alpha,\beta,\gamma) \ , \tag{B4}$$

where identities from Ref. 15 have been employed. Thus

$$\Psi_{RV} = \frac{1}{r_1 r_2} R_{v_1 v_3}(r_1, r_2) G_{v_2}^k(\theta_{12})$$

$$\times \left[\frac{2J+1}{8\pi^2} \right]^{1/2} \frac{(2-\delta_{k0})^{1/2}}{2}$$

$$\times [\mathcal{D}_{Mk}^{J*}(\alpha\beta\gamma) + (-1)^{J+S+v_3} \mathcal{D}_{M-k}^{J*}(\alpha\beta\gamma)] \ . \quad \text{(B5)}$$

This wave function has a definite parity which we determine by applying the inversion operator $\hat{P}$,

$$\hat{P} \mathcal{D}_{Mk}^J(\alpha, \beta, \gamma) = \mathcal{D}_{Mk}^J(\alpha, \pi + \beta, 2\pi - \gamma) \quad \text{(B6)}$$

$$= (-1)^{J+k} \mathcal{D}_{M-k}^J(\alpha, \beta, \gamma) \ , \quad \text{(B7)}$$

where again identifies from Ref. 15 have been used. Thus it follows that

$$\hat{P} \Psi_{RV} = (-1)^{k+S+v_3} \Psi_{RV} \ . \quad \text{(B8)}$$

Now turning to the atomic CI wave function [Eq. (9)], we have

$$\hat{P} \Psi_{CI} = (-1)^{l_1 + l_2} \Psi_{CI} \ . \quad \text{(B9)}$$

Also,

$$\hat{P}_{12} \mathcal{Y}_{l_1 l_2}^{LM}(\hat{r}_1, \hat{r}_2)$$

$$= (-1)^{l_1 + l_2 + L} \mathcal{Y}_{l_2 l_1}^{LM}(\hat{r}_1, \hat{r}_2) \quad \text{(B10)}$$

$$= (-1)^{l_1 + l_2 + M} \sum_K F_{l_1 l_2}^{LK}(\theta_{12}) \mathcal{D}_{-MK}^L(\alpha, \beta, \gamma) \quad \text{(B11)}$$

where the first step follows from symmetry relations for the Clebsch-Gordan coefficients and the second from Eqs. (12) and (A5). Thus overall

$$\Psi_{CI} = \frac{(-1)^M}{\sqrt{2}} \sum_{l_1 n_1 l_2 n_2} C_{l_1 n_1 l_2 n_2} \sum_K F_{l_1 l_2}^{LK}(\theta_{12}) \mathcal{D}_{-MK}^L(\alpha, \beta, \gamma)(-1)^K [\phi_{n_1 l_1}(r_1)\phi_{n_2 l_2}(r_2) + (-1)^{l_1 + l_2 + S + K} \phi_{n_2 l_2}(r_1)\phi_{n_1 l_1}(r_2)] \ . \quad \text{(B12)}$$

The projection is given by

$$\int \Psi_{RV}^* \Psi_{CI} d\tau \ , \quad \text{(B13)}$$

where

$$d\tau = r_1^2 dr_1 r_2^2 dr_2 \sin\theta_{12} d\theta_{12} d\alpha \sin\beta d\beta d\gamma \ . \quad \text{(B14)}$$

We need the transformation[15]

$$[\mathcal{D}_{Mk}^{J*}(\alpha, \beta, \gamma)]^* = (-1)^{M+k} \mathcal{D}_{-M-k}^{J*}(\alpha, \beta, \gamma) \ . \quad \text{(B15)}$$

Now, using the expression for the integral of a product of rotation matrices,[15] the integral over the Euler angles may be evaluated with the result

$$\int_0^{2\pi} d\alpha \int_0^\pi \sin\beta d\beta \int_0^{2\pi} d\gamma [\mathcal{D}_{-M-k}^{J*}(\alpha\beta\gamma) + (-1)^{J+S+v_3} \mathcal{D}_{-Mk}^{J*}(\alpha\beta\gamma)] \mathcal{D}_{-MK}^L(\alpha\beta\gamma)$$

$$= \frac{8\pi^2}{2L+1} \delta_{LJ} [\delta_{K-k} + (-1)^{L+S+v_3} \delta_{Kk}] \ . \quad \text{(B16)}$$

Thus the only $F_{l_1 l_2}^{LK}(\theta_{12})$ term that survives the sum over K is

$$F_{l_1 l_2}^{L-k}(\theta_{12}) + (-1)^{L+S+v_3} F_{l_1 l_2}^{Lk}(\theta_{12}) = [(-1)^{l_1 + l_2 + L + k} + (-1)^{L+S+v_3}] F_{l_1 l_2}^{Lk}(\theta_{12}) \quad \text{(B17)}$$

$$= (-1)^{L+k}(\pi_a + \pi_m) F_{l_1 l_2}^{Lk}(\theta_{12}) \quad \text{(B18)}$$

$$= (-1)^{L+k} 2\pi_a \delta_{\pi_a \pi_m} F_{l_1 l_2}^{Lk}(\theta_{12}) \ , \quad \text{(B19)}$$

where π_a and π_m are the parities of the atomic and molecular wave functions, respectively, and Eq. (A6) has been used. Combining this last equation with those above, Eq. (15) follows immediately.

[1]R. P. Madden and K. Codling, Phys. Rev. Lett. **10**, 516 (1963).

[2]J. W. Cooper, U. Fano, and F. Prats, Phys. Rev. Lett. **10**, 518 (1963).

[3]C. D. Lin, Phys. Rev. A **29**, 1019 (1984).

[4]M. E. Kellman and D. R. Herrick, Phys. Rev. A **22**, 1536 (1980).

[5]D. R. Herrick, M. E. Kellman, and R. D. Poliak, Phys. Rev. A **22**, 1517 (1980).

[6]S. Watanabe and C. D. Lin, Phys. Rev. A **34**, 823 (1986).

[7]M. E. Kellman and D. R. Herrick, J. Phys. B **11**, L755 (1978).

[8]H.-J. Yuh, G. S. Ezra, P. Rehmus, and R. S. Berry, Phys. Rev. Lett. **47**, 497 (1981).

[9]G. S. Ezra and R. S. Berry, Phys. Rev. A **28**, 1974 (1983).

[10]M. E. Kellman, Phys. Rev. Lett. **55**, 1738 (1985).

[11]J. L. Krause and R. S. Berry, J. Chem. Phys. **83**, 5153 (1985).

[12]C. H. Townes and A. L. Schawlow, *Microwave Spectroscopy* (Dover, New York, 1975).

[13]M. D. Morse, K. F. Freed, and Y. B. Band, J. Chem. Phys. **70**, 3604 (1979).

[14]J. I. Steinfeld, *Molecules and Radiation* (Harper and Row, New York, 1974).

[15]D. M. Brink and G. R. Satchler, *Angular Momentum* (Clarendon, Oxford, 1968).

[16]I. S. Gradshteyn and I. M. Ryzhik, *Table of Integrals, Series, and Products* (Academic, New York, 1965).

[17]S. I. Nikitin and V. N. Ostrovsky, J. Phys. B **18**, 4349 (1985).

[18]H. C. Allen and P. C. Cross, *Molecular Vib-Rotors* (Wiley, New York, 1963).

[19]W. C. Martin, J. Phys. Chem. Ref. Data **2**, 257 (1973).

[20]C. E. Moore, *Atomic Energy Levels,* Natl. Bur. Stand. (U.S.) Circ. No. 467 (U. S. GPO, Washington, D. C. 1949), Vol. I; *ibid.* (U. S. GPO, Washington, D. C., 1952), Vol. II.

[21]R. T. Lawton and M. S. Child, Mol. Phys. **40**, 773 (1980).

[22]P. M. Morse, Phys. Rev. **34**, 57 (1929).

[23]P. C. Ojha and R. S. Berry, Phys. Rev. A **36**, xxx (1987).

[24]R. S. Berry and J. L. Krause, Phys. Rev. A **33**, 2865 (1986).

[25]S. I. Nikitin and V. N. Ostrovsky, J. Phys. B **9**, 3141 (1976); **11**, 1681 (1978).

[26]A. R. Edmonds, *Angular Momentum in Quantum Mechanics* (Princeton University, Princeton, N.J., 1960).